

PREDICTIVE ADAPTIVE FEEDFORWARD CONTROL OF A TIME SCALED SOLAR PLANT

R. N. Silva and J. M. Lemos

DEE-FCT/UNL, 2829-516 Caparica, Portugal,

rns@mail.fct.unl.pt

INESC-ID/IST, R. Alves Redol, 9, Lisboa

jlm@inesc-id.pt

Abstract: This paper concerns the control of a solar energy collector field using predictive feedforward adaptive control techniques based on multiple identifiers. The ACUREX field used in these work is described by a partial differential equation (PDE). The plant is characterized by: non linearity, fast accessible disturbances and time varying dynamics. The dynamic dependency on flow is overcome by time-scaling. The result of this transformation is a discrete linear model with a Finite Impulse Response (FIR) transfer function. This means that the optimal predictive controller is given by a feedforward block. Simulation results on a detailed plant physical model are presented in order to illustrate the method. *Copyright ©2005 IFAC.*

Keywords: Time-scaling, adaptive control, predictive control, solar energy.

1. INTRODUCTION

This paper concerns the control of a solar energy collector field and extends the work presented in (Coito et al., 1997) using predictive adaptive control techniques based on multiple identifiers by using time varying sampling.

The ACUREX field used in these work is described in the available literature (Camacho et al., 1992; Camacho et al., 1988). In this plant the main sources of disturbances are measured and its dynamic behaviour depends strongly on its geometry (available). This allows us to derive an accurate model which is described by a partial differential equation (PDE). The plant is characterized by: non linearity caused by the dependency of bandwidth and static gain with flow (the manipulated variable); fast accessible disturbances (solar radiation with sudden clouds); time varying dynamics with the daily and annually cycles, and pluvial cycles that modify the reflectivity of the mirrors; and sudden plant changes when groups of collectors are entering/exiting solar track.

Due to this strong non-linear behaviour, the use of predictive adaptive algorithms based on linear models is limited on the operating point rate of change. A best compromise between the tracking

capabilities of the adaptive controller and its sensitivity to disturbances should be found resulting in a sub-optimal solution.

With the objective of overcoming this tie, a time scaling transformation in the discretization procedure was proposed in (Silva, 1999) and further exploited in (Silva and Lemos, 2001; Silva et al. 2003a; Silva et al. 2003b). Since the controller is to be implemented in a digital computer, the dynamic dependency on flow can be overcome by time-scaling, replacing the elements of time (sampling period) by elements of volume. The result of this transformation is a discrete linear model (the variable sampling period dependent on the imposed flow) with a Finite Impulse Response (FIR) transfer function. This means that the optimal predictive controller is given by a feedforward block with the inputs: setpoint value, accessible disturbances and past control actions, *i.e.* there is no dependency on the plant output.

The work presented in this paper exploits the Feedforward version of the MUSMAR algorithm together with time-scaling methods in the control of a plant with transport phenomena. Plants, such as rolling mills, conveyor belts or fluids in pipes can be transformed with time-scaling (Åström and

Wittenmark, 1984). Plants of this class may be controlled with advantage using the method reported here. The paper is organized as follows. In section 2 the plant and the discretization of its the non linear model is described. Section 3 describes the time-scaled discretization procedure. The convergence properties of the proposed controller are presented in Section 4. In section 5 some simulation results on the full-scale plant model are shown and some conclusions are drawn in section 6.

2. PLANT DESCRIPTION AND MODEL

The ACUREX field of the Plataforma Solar de Almería (PSA) in Southern Spain, consists of 480 distributed solar collectors. They are arranged in 10 loops along an east-west axis (fig. 1). The collector has a reflective cylindrical parabolic surface in order to concentrate the incident solar radiation on a pipe located on the surface focal line. A heat transfer fluid (oil) is pumped from the bottom of a storage tank through the collectors, where it collects solar energy, and from the output of the field, again to the top of the tank. By manipulating the oil flow, with the pump, it is possible to control the output temperature of the oil. values of an array of 10 temperature sensors located at the output of each loop. Due to safety reasons the oil flow is limited between 2.0 and 10.0 liters per second. The heated oil from the collector field stored in the tank can be used e.g. for the production of electrical energy or for the operation of a desalination plant. The field is equipped with a tracking system by which the mirrors can rotate parallel to the axis of the receiving tube in order to follow the sun in height throughout the day. There is a temperature sensor located at the input of the field, measuring the temperature of the oil entering the active part (mirrors). It is also available a 2 d.o.f. solar radiation sensor that is able to follow the sun, measuring the total incident radiation. With an algorithm using the actual day and time it is possible to compute the corrected radiation (i.e. the effective radiation heating the oil) from that measure.



Fig.1 ACUREX Solar collector field.

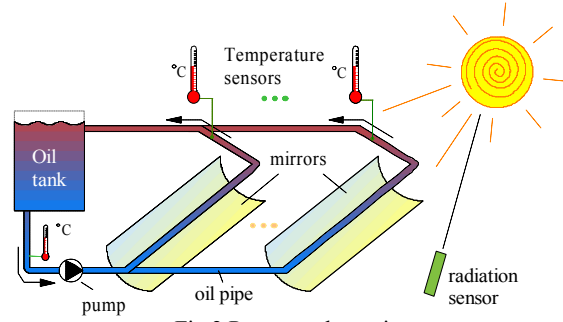


Fig.2 Process schematic.

The focus of the modelling work has been put into the transport effect since this is the most relevant part for the dynamics. Other thermal mechanisms, such as e.g. thermal diffusion, have been neglected in the model presented next (Pickhardt and Silva, 1998). The model is nonlinear, yet, it is given by a simple formula with only two parameters that relates the output temperature T_{out} , with the input temperature T_{in} , and the solar radiation R :

$$T_{out}(t) = \Psi \cdot T_{in}(t - \mathbf{t}) + \Gamma \int_{t-\mathbf{t}}^t R(\mathbf{s}) d\mathbf{s} \quad (1)$$

The parameter $\Gamma = (Dh_o)/(rAS_f)$ where D is the mirrors width, h_o is the optical efficiency, A is the transversal pipe section area, S_f is the specific thermal capacity of the oil and r is the oil density approximated by a constant) has been estimated using real plant data and the same was made for the parameter Ψ that takes into account the losses inside the collector. The input-output travelling time, \mathbf{t} , is obtained from

$$\int_{t-\mathbf{t}}^t F(\mathbf{s}) d\mathbf{s} = V \quad (2)$$

where $F(\cdot)$ is the volumetric flow inside the collector and V is the total collector volume.

3. TIME SCALED DISCRETIZATION

The controller developed in this work results from the minimization of a quadratic cost over an extended horizon based on the model described in the previous section after time scaled discretization. Consider again equations (1) and (2) and use elementary volumes instead of elementary time intervals (sampling period) on a discretization procedure. Thus, let us divide de collector volume V in n smaller equal volumes v and consider a zero order hold (ZOH) for the flow command since the controller will be implemented in a digital computer.

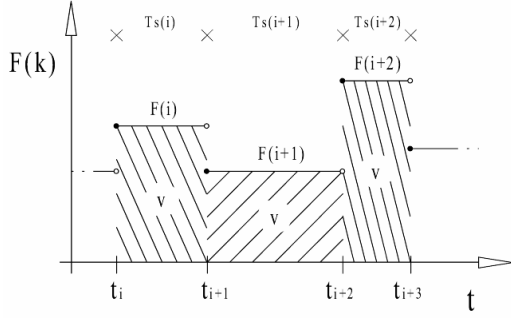


Fig.3 Relation between flow and sampling periods.

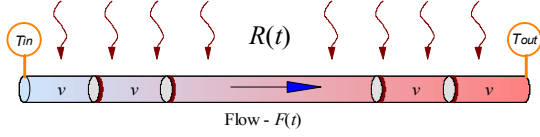


Fig.4 Active part volume division.

Choose the sampling period T_s for each discrete time instant, k , such that the product of the flow value by the sampling period results in the elementary volume (fig. 4) i.e.

$$F(k) \times T_s(k) = v = \frac{V}{n} \quad (3)$$

Then, equation (3) implies that

$$\sum_{i=1}^n T_s(k-i) = \mathbf{t}_k \quad (4)$$

where \mathbf{t}_k stands for the I/O transport delay (through volume V), in seconds, for the fluid element that is present at time instant k at the output. The discrete time radiation signal can be computed from the continuous one with a forward average at time k as

$$R(k) = \frac{1}{T_s(k)} \int_{t_k}^{t_{k+1}} R(s) ds \quad (5)$$

Then, equation (1) becomes, in a discrete version,

$$T_{out}(k) = \Psi \cdot T_{in}(k-n) + \Gamma \sum_{i=k-n}^{k-1} R(i) T_s(i) \quad (6)$$

Defining $u(k) = F(k)^{-1}$ as the new control variable, from (3) and (6) we get

$$T_{out}(k) = \Psi \cdot T_{in}(k-n) + \mathbf{a} \sum_{i=k-n}^{k-1} R(i) u(i) \quad (7)$$

where $\mathbf{a} = \Gamma \times v$. Equation (7) is a non-recursive discrete linear system (entirely feedforward) with time varying coefficients depending on the radiation signal.

4. THE FEEDFORWARD MUSMAR ADAPTIVE PREDICTIVE CONTROLLER

The MUSMAR controller [Greco *et al.*, 84, Mosca, 95] is based on a number of separately estimated predictive models. In the presence of plant/model mismatches, such as the situations found here, the redundancy thereby introduced proves important for achieving a correct control action [Mosca *et al.*, 89]. This multiple model approach is a distinctive feature with respect to other approaches to predictive adaptive control, relying on the adaptation of a single model from which others are then obtained. In [Greco *et al.*, 84] it is shown that MUSMAR is equivalent to a bank of parallel self-tuners, each one tuned to a different value of plant delay and with different weights. If the actual plant delay is bigger than the delay assumed for a given self-tuning channel the corresponding weight will be zero. Insensitivity to uncertainty in plant delay is thus achieved up to some degree.

FF-MUSMAR algorithm

The MUSMAR algorithm reads as follows:

At the beginning of each sampling interval k (discrete time), recursively perform the following steps:

1. Sample plant output, $y(k)$ and compute the tracking error \tilde{y} , with respect to the desired setpoint $r(k)$ by:

$$\tilde{y}(k) = r(k) - y(k) \quad (8)$$

2. Using Recursive Least Squares (RLS), update the estimates of the parameters \mathbf{q}_j , \mathbf{y}_j , \mathbf{m}_{j-1} and \mathbf{f}_{j-1} the following set of predictive models:

$$\tilde{y}(k+j) \approx \mathbf{q}_j u(k) + \mathbf{y}_j^T s(k) \quad (9)$$

$$u(k+j-1) \approx \mathbf{m}_{j-1} u(k) + \mathbf{f}_{j-1}^T s(k) \quad (10)$$

$$j = 1 \dots N$$

where \approx denotes equality in least squares sense and $s(k)$ is a sufficient statistic for computing the control, hereafter referred as the pseudo-state, given by

$$s(k) = [u(k-1) \dots u(k-n_B) w(k) \dots w(k-n_w)]^T \quad (11)$$

where the $w(k)$ are samples from accessible disturbances in order to provide the feedforward action. Since, at time k , $\tilde{y}(k+j)$ and $u(k+j)$ are not available for $j \geq 1$, for the purpose of estimating the parameters, the variables in (9,10) are

delayed in block of N samples. The estimation equations are thus,

$$K(k) = \frac{P(k-1)\mathbf{j}(k-N)}{1 + \mathbf{j}^T(k-N)P(k-1)\mathbf{j}(k-N)[1 - \mathbf{b}(k)]} \quad (12)$$

$$P(k) = [I - K(k)\mathbf{j}^T(k-N)(1 - \mathbf{b}(k))]P(k-1) \quad (13)$$

and

$$\hat{\Theta}_j(k) = \hat{\Theta}_j(k-1) + K(k)\mathbf{e}_j(k) \quad (14)$$

$\mathbf{e}_j(k) = \tilde{y}(k-N+j) - \hat{\Theta}_j^T(k-N)\mathbf{j}(k-N)$
with $j = 1 \cdots N$; and for $j = 1 \cdots N-1$

$$\hat{\Omega}_j(k) = \hat{\Omega}_j(k-1) + K(k)\mathbf{d}_j(k) \quad (15)$$

In these equations, $\hat{\Theta}_j$ represents the estimate of the parameter vector of the output predictors, given at each discrete time and for each predictor j by

$$\hat{\Theta}_j = [\mathbf{q}_j \quad \mathbf{y}_j^T]^T$$

and $\mathbf{j}(k-N)$ represents the regressor, common to all predictors, given by

$$\mathbf{j}(k-N) = [\mathbf{u}(k-N) \quad \mathbf{s}^T(k-N)]^T$$

Similarly, $\hat{\Omega}_j$ represents the estimate of the parameter vector of the input predictors, given at each discrete time and for each predictor j by

$$\hat{\Omega}_j = [\mathbf{m}_j \quad \mathbf{f}_j^T]^T$$

Note that, since the regressor $\mathbf{j}(k-N)$ is common to all the predictive models, the Kalman gain update (12) and the covariance matrix update (13) are also common to all the predictors and need to be performed only once per time iteration. This greatly reduces the computational load.

3. Apply to the plant the control given by

$$\mathbf{u}(k) = \mathbf{f}^T \mathbf{s}(k) + \boldsymbol{\eta}(k) \quad (16)$$

where $\boldsymbol{\eta}$ is a white dither noise of small amplitude and \mathbf{f} is the vector of controller gains, computed from the estimates of the predictive models by

$$\mathbf{f} = -\frac{1}{a} \left(\sum_{i=1}^N \theta_j \boldsymbol{\psi}_j + \rho \sum_{i=1}^{N-1} \boldsymbol{\mu}_j \boldsymbol{\phi}_j \right) \quad (17)$$

with the normalization factor a given by

$$a = \sum_{i=1}^N \mathbf{q}_j^2 + \mathbf{r} \left(1 + \sum_{i=1}^{N-1} \mathbf{m}_j^2 \right) \quad (18)$$

4. CONVERGENCE PROPERTIES OF THE FEEDFORWARD MUSMAR

Consider a plant described by the following ARMAX with accessible disturbance model

$$A(q)y(k) = B(q)u(k) + C(q)e(k) + D(q)w(k) \quad (19)$$

where q is the forward shift operator, y is the plant output, u is the plant input (manipulated variable), $\{e(k)\}$ is a sequence of independent, identically distributed (i.i.d.) random variables with zero mean and finite variance and $\{w(k)\}$ is an accessible disturbance modelled by a sequence of i.i.d. random variables independent of $\{e(k)\}$ and such that $E\{w(k)w(k+t)\} = \mathbf{d}_t \mathbf{s}_w^2$, where \mathbf{d}_t is Kronecker symbol. In the special case where $A(q)$ is Hurwitz, the vector gain \mathbf{f} of the reduced complexity feedforward controller

$$\mathbf{u}(k) = \mathbf{f}^T \mathbf{s}(k) \quad (20)$$

is to be adjusted such as to minimize the steady-state quadratic cost

$$J(\mathbf{f}) = \lim_{k \rightarrow \infty} E\{\tilde{y}^2(k) + \rho u^2(k)\} \quad (21)$$

In the presence of the controller (20) written in the form of a rational transfer function

$$T(q)u(k) = -M(q)w(k) \quad (22)$$

the optimal feedforward controller is characterized as follows. Replacing (22) in (19) yields ($e(k) = 0$)

$$y(k) = \left(\frac{D(q)T(q) - B(q)M(q)}{A(q)T(q)} \right) w(k) \quad (23)$$

Following the same approach as in (Mosca et al, 1989) it can be shown that

$$\frac{\partial y(k, \mathbf{f})}{\partial \mathbf{f}} = \frac{B(q)}{A(q)T(q)} \mathbf{s}(k) \quad (24)$$

$$\frac{\partial u(k, \mathbf{f})}{\partial \mathbf{f}} = \frac{1}{T(q)} \mathbf{s}(k) \quad (25)$$

where for

$$\mathbf{f} = [-t_1 \cdots -t_{n_B} \quad -m_0 \cdots -m_{n_W}]^T$$

the gradient (24) of the output $y(k, \mathbf{f})$ with respect to \mathbf{f} is given by

$$\frac{\partial y(k, \mathbf{f})}{\partial \mathbf{f}} = \left[-\frac{\partial y(k, \mathbf{f})}{\partial t_1} \cdots -\frac{\partial y(k, \mathbf{f})}{\partial t_{n_B}} \cdots \right] \quad (26)$$

being (25) defined in an analogous way.

The minimization of (21) gives

$$\frac{\partial J(\mathbf{f})}{\partial \mathbf{f}} = E \left\{ y(k) \frac{\partial y(k)}{\partial \mathbf{f}} + \rho u(k) \frac{\partial u(k)}{\partial \mathbf{f}} \right\} = 0 \quad (27)$$

and replacing (24) and (25) yields

$$E \left\{ y(k) \left(\frac{B(q)}{A(q)T(q)} \mathbf{s}(k) \right) + \rho u(k) \left(\frac{1}{T(q)} \mathbf{s}(k) \right) \right\} = 0 \quad (28)$$

In order to compute the equilibrium gain yielded by Feedforward MUSMAR, the approximation is made of assuming that the plant is being controlled since the remote past and from $i = k$ up to $k + N - 1$ by a control law of the form

$$u(i) = f_0^T s(i) + \eta(i) \quad (29)$$

where f_0 is a stabilizing constant vector gain and $\{h(i)\}$ is a low power dither noise independent of $\{s(i)\}$ and such that

$$\begin{aligned} E\{h(i)\} &= 0 \\ E\{h(i)h(i+j)\} &= \mathbf{d}_j \mathbf{s}_h^2 \end{aligned} \quad (30)$$

Due to the assumptions made, the output of the plant admits least-squares predictors of the form (19,20). The Feedforward MUMAR algorithm is analysed using the ODE method (Mosca et al, 1989). The following set of ODEs can be associated with the FF-MUMAR

$$\begin{bmatrix} \dot{\mathbf{q}}_j(\mathbf{t}) \\ \dot{\mathbf{y}}_j(\mathbf{t}) \end{bmatrix} = R_z^{-1}(\mathbf{t}) E\{z(k)[y(k+j) - (\mathbf{q}_j(\mathbf{t})u(k) + \mathbf{y}_j^T(\mathbf{t})s(k))]\} \quad (31)$$

$$\begin{bmatrix} \dot{\mathbf{m}}_{j-1}(\mathbf{t}) \\ \dot{\mathbf{f}}_{j-1}(\mathbf{t}) \end{bmatrix} = R_z^{-1}(\mathbf{t}) E\{z(k)[u(k+j-1) - (\mathbf{m}_{j-1}(\mathbf{t})u(k) + \mathbf{f}_{j-1}^T(\mathbf{t})s(k))]\} \quad (32)$$

$$\dot{R}_z(\mathbf{t}) = E\{z(k)z^T(k)\} - R_z(\mathbf{t}) \quad (33)$$

where $z(k) = [u(k) \quad s^T(k)]^T$ and (\cdot) denotes the derivative operator with respect to \mathbf{t} .

Replacing the control input of (27) in the equations (31,33) and since $E\{h(k)s(k)\} = 0$, at equilibrium

$$\mathbf{q}_j^* = \frac{E\{h(k)y(k+j)\}}{\mathbf{s}_h^2} \quad (34)$$

$$\mathbf{m}_{j-1}^* = \frac{E\{h(k)u(k+j-1)\}}{\mathbf{s}_h^2} \quad (35)$$

Again from equations (31,33), it is possible to write, at equilibrium, the following equation

$$\begin{aligned} & E\left\{s(k) \sum_{j=1}^N \mathbf{q}_j y(k+j) + \mathbf{r} \mathbf{m}_{j-1} u(k+j-1)\right\} \\ & - E\left\{s(k) \sum_{j=1}^N [\theta_j^2 + \rho \mu_{j-1}^2] \eta(k)\right\} + E\left\{s(k) \left[\left(\sum_{j=1}^N \theta_j^2 + \rho \sum_{j=1}^N \mu_{j-1}^2 \right) f \right. \right. \\ & \left. \left. + \sum_{j=1}^N \mathbf{q}_j \mathbf{y}_j + \mathbf{r} \mathbf{m}_{j-1} \mathbf{f}_{j-1} \right]\right\} = 0 \end{aligned} \quad (36)$$

The second and (by (17)) the third terms are null implying for the first term (after reordering)

$$E\left\{y(k) \sum_{j=1}^N \mathbf{q}_j s(k-j) + \mathbf{r} u(k) \sum_{j=1}^N \mathbf{m}_{j-1} s(k-j+1)\right\} = 0 \quad (37)$$

If $H(q)|_N$ represents the $H(q)$ filter truncated to its first N impulse response samples, from (34,35), at equilibrium

$$E\left\{y(k) \left(\frac{B(q)}{A(q)T(q)} \right)_N s(k) + \mathbf{r} u(k) \left(\frac{1}{T(q)} \right)_N s(k)\right\} = 0 \quad (38)$$

Comparing this solution with (28) it is concluded that when $N \rightarrow \infty$ the equilibrium gain yielded by the FF-MUSMAR approaches the optimal solution defined by (28) when $k \rightarrow \infty$.

Additionally, it is possible to show (see Mosca et al, 1989) that the ODE correspondent to $f(\tau)$ can be written as

$$\dot{f} = -\frac{1}{\alpha} R_s^{-1} \nabla_N J(f) + o(|f - f^*|) \quad (39)$$

where f^* denotes any equilibrium point, $R_s = E\{s(k)s^T(k)\}$ and $o(|x|)$ is such that $\lim_{x \rightarrow 0} o(|x|)/|x| = 0$.

This means that if N is large enough, close to the equilibrium, FF-MUSMAR updates the controller vector gain according to the gradient of the cost function.

5. SIMULATION RESULTS WITH THE SOLAR FIELD

The following simulations were performed using the model from equations (1,2) with $n = 10$. For a total volume of 1800 liters, this gives a value of the elementary volume $v = 180 \text{ l}$.

The simulation was performed with the following parameters:

$$N = 10 \quad \mathbf{r} = 0.01 \quad \mathbf{l} = 0.985 \quad \mathbf{s}_h^2 = 2 \times 10^{-2}$$

$$n_B = 3 \quad n_R = 1 \quad n_W = 2 \quad P(0) = 10^3$$

where n_R is the number of reference terms in the pseudo-state, making an additional feedforward action from the set-point changes, which are also disturbances on the system.

The simulation starts with zero knowledge in the predictor models and the controller is purely feedforward since there is no feedback term in the pseudo-state $s(k)$. For simulation purpose the time is represented in hours in order to establish the radiation curve around solar noon. Additionally, two variations were performed on the inlet temperature value. Figure 5 show the output temperature and

reference value and manipulated flow. The radiation and the input temperature are depicted in figure 6. In figure 7 the FF-MUSMAR vector gain is represented.

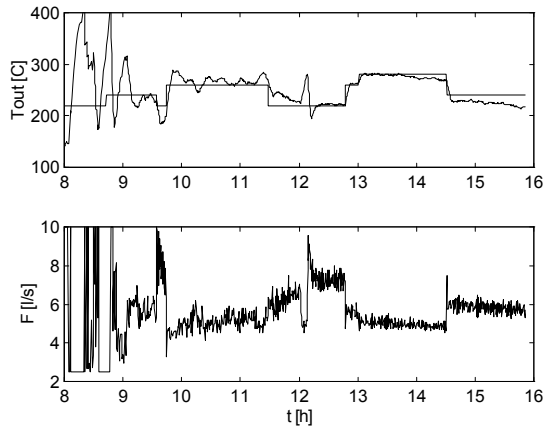


Fig.5 Output temperature (top) and flow (bottom).

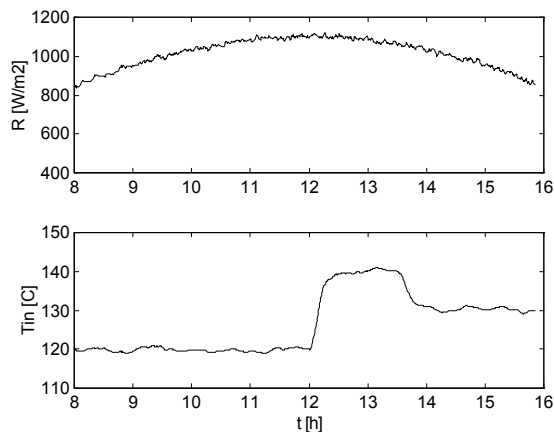


Fig.6 Radiation (top) and input temperature (bottom).

6. CONCLUSIONS

This paper shows how MUSMAR, a predictive adaptive control algorithm based on multiple identifiers in its feedforward version, can be used to tackle a problem that arises from the time-scaled discretization of a distributed parameter system. The Finite Impulse Response structure of the plant model after discretization results in controller purely feedforward, the uncertainty being compensated by the adaptive nature of the control algorithm.

REFERENCES

Coito F., J.M. Lemos, R. N. Silva and E. Mosca (1997). "Adaptive control of a solar energy plant: exploiting acceptable disturbances." *Int. Journal of Adaptive Control and Signal Proc.*, **11**, 327-342.

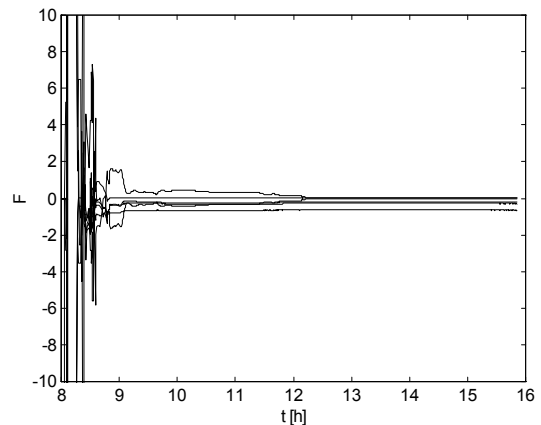


Fig.7 FF-MUSMAR controller gains.

Aström, K., and B.Wittenmark (1989). *Adaptive Control*. Addison Wesley.

Mosca, E. (1995). *Optimal, Predictive, and Adaptive Control*, Prentice Hall.

Silva, R. N., (1999). Time scaled predictive controller of a solar power plant, V European Control Conference 99, Karlsruhe, Germany.

Silva, R. N., J. M. Lemos (2001). Adaptive control of transport systems with non-uniform sampling. VI European Control Conf., Oporto, Portugal.

Silva, R. N., L. M. Rato e J. M. Lemos (2003). Time scaling internal state predictive control of a solar plant. *Control Engineering Practice*, 11, 12, 1459-1467.

Silva, R. N., J. M. Lemos e L. M. Rato (2003). Variable sampling adaptive control of a distributed collector solar field. *IEEE Trans. Control Systems Technology*, 11, 5, 765-772.

Pickhardt, R., and R. N. Silva (1998). Application of a nonlinear predictive controller to a solar power plant. *Proc. 1998 IEEE-CCA*, Trieste, Italy.

Camacho, E.; F. Rubio and F. Hughes (1992). Self-tuning control of a solar power plant with a distributed collector field, *IEEE Control Systems Mag.*, pp. 72-78, April 92.

Camacho, E.; F. Rubio and J. Gutierrez (1988). Modelling and simulation of a solar power plant with distributed collector system, *IFAC Symp. On Power Systems Modelling and Control Applications*, Brussels, Belgium.

Greco, C., G. Menga, E. Mosca and G. Zappa (1984). Performance Improvements of Self-tuning Controllers by Multistep Horizons: The MUSMAR Approach. *Automatica*, 20:681-699.

Mosca, E. G. Zappa. and J.M. Lemos (1989). "Robustness of multipredictor adaptive regulators: MUSMAR" *Automatica*, 25:521 - 529.